CHALMERS
UNIVERSITY OF TECHNOLOGY

Programmable Filterless Optical Networks: Architecture, Design and Resource Allocation

Programmable Filterless Optical Networks: Architecture, Design and Resource Allocation

Ehsan Etezadi, *Graduate Student Member, IEEE,* Carlos Natalino, *Member, IEEE,* Christine Tremblay, *Senior Member, IEEE,* Lena Wosinska, *Senior Member, IEEE,* and Marija Furdek, *Senior Member, IEEE*

***Abstract*—Filterless optical networks (FONs) are a cost-effective optical networking technology that replaces reconfigurable optical add-drop multiplexers, used in conventional, wavelength-switched optical networks (WSONs), by passive optical splitters and couplers. FONs follow the *drop-and-waste* transmission scheme, i.e., broadcast signals without filtering, which generates spectrum waste. Programmable filterless optical networks (PFONs) reduce this waste by equipping network nodes with programmable optical white box switches that support arbitrary interconnections of passive elements. Cost-efficient PFON solutions require optimal routing, modulation format and spectrum assignment (RMSA) to connection requests, as well as optimal design of the node architecture. This paper presents an optimization framework for PFONs. We formulate the RMSA problem in PFONs as a single-step integer linear program (ILP) that jointly minimizes the total spectrum and optical component usage. As RMSA is an NP-complete problem, we propose a two-step ILP formulation that addresses the RMSA sub-problems separately and seeks sub-optimal solutions to larger problem instances in acceptable time. Simulation results indicate a beneficial trade-off between component usage and spectrum consumption in proposed PFON solutions. They use up to 64% less spectrum than FONs, up to 84% fewer active switching elements than WSONs, and up to 81% fewer optical amplifiers at network nodes than FONs or WSONs.**

***Index Terms*—Filterless optical networks; coherent elastic transmission; optical white box; wavelength routing; mathematical programming.**

I. Introduction

To support the immense traffic growth and enable scalable on-demand provisioning of service requests, optical networks must deliver great adaptability in a cost- and resource-efficient manner. Agile and flexible optical networking can be achieved in different ways through different technological solutions. The most relevant functionalities enabling adaptable optical networks refer to programmability and reconfigurability of optical switches and edge terminals, which can then be combined into diverse solutions with different trade-offs between performance and cost.

In conventional wavelength-switched optical networks (WSONs), nodes deploy reconfigurable optical add-drop multiplexers (ROADMs) with hard-wired constituent components that support transparent switching of optical signals based on their wavelength, as well as local add and drop at the node. An unprecedented level of flexibility in nodal architecture design and network provisioning is provided by disaggregated optical white boxes, also referred to as architecture on demand (AoD) or function programmable switches [1]. Unlike hard-wired ROADMs, white boxes do not interconnect optical modules (e.g., wavelength-selective switches, passive couplers or erbium-doped fiber amplifiers (EDFAs)) in a fixed manner. Instead, the modules are interconnected via an optical backplane (OB) (e.g., piezoelectric space switch [2]). This allows to efficiently satisfy the traffic requirements (every connection uses only the required modules) and enables swift reconfiguration in order to accommodate traffic changes, scale capacity, or upgrade the network. Consequently, AoD brings benefits in terms of cost- and energy-efficiency, scalability, and network reliability compared to their ROADM-based counterpart [1].

Filterless optical networks (FONs) have been proposed as a low-cost solution for agile optical networking [3], and accepted as a viable technological solution for deployments in core and metro networks with feasibility demonstrated through several pilot trials. Nodes in FONs use only passive components (i.e., optical couplers and splitters) to broadcast signals, without any active switching or filtering. These passive interconnects result in a set of passive fiber trees that carry signals across the network, while tunable elastic coherent transmitters and receivers at the edge nodes support agile operation [4]. Transmission in FONs follows the *drop-and-waste* principle, where signals are broadcasted to all links in the fiber tree downstream of the source node and continue to propagate along the links beyond the destination node due to the absence of filtering. The inherently gridless arhitecture and the absence of active switching components bring major advantages of FONs in terms of cost-effectiveness, reliability and energy-efficiency [3]. However, these benefits come at the expense of higher spectrum usage due to the *drop-and-waste* transmission, as well as a rigid physical structure with no architectural flexibility.

To mitigate the drawbacks and combine the benefits of filterless networking with the advantages of optical white boxes, a programmable filterless optical network (PFON) architecture based on optical white boxes was proposed in [5]. The underlying idea of PFONs is to keep the gridless nature and line system simplifications enabled by filterless networking while introducing node architecture flexibility supported by AoD nodes. Such flexibility enables better adaptation of the nodal

Manuscript received 29 April, 2022; revised 22 March, 2023; accepted 17 August 2023. This research was supported in part by Compute Canada (www.computecanada.ca). *(Corresponding author: Marija Furdek.)*

E. Etezadi, C. Natalino, L. Wosinska and M. Furdek are with the Department of Electrical Engineering, Chalmers University of Technology, 412 96 Gothenburg, Sweden. e-mail: furdek@chalmers.se.

C. Tremblay is with École de technologie supérieure, Montréal, QC H3C 1K3, Canada.

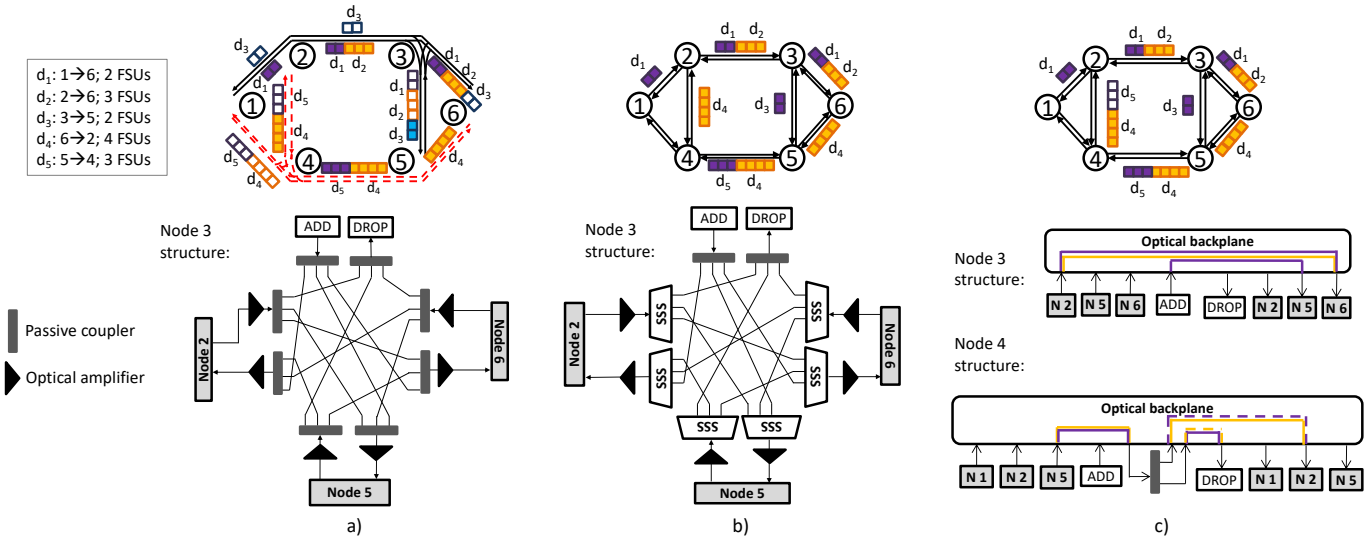

Figure 1. An illustrative example of (a) passive filterless, (b) conventional wavelength-switched, and (c) programmable filterless optical network architecture supporting five connection requests, along with the configuration of representative nodes shown below.

configuration to the traffic demands, yielding lower dissipation of spectrum due to the *drop-and-waste* transmission. The PFON architecture is illustrated in Fig. 1 through comparison to FON and WSON, using a simple network example with 6 nodes and 5 communication demands denoted by d_1 to d_5.

Fig. 1a depicts a fully passive filterless solution where two passive fiber trees (shown with the full black and the dashed red lines, respectively) connect the nodes. The details of the internal structure are shown for node 3 below the network example and are analogous for all other nodes. Each node comprises passive splitters and couplers. The nodes also host amplifiers at each ingress and egress port, referred to as pre-amplifiers and boosters, respectively. The absence of filtering implies that a copy of each signal present at the input port of a passive splitter also appears on all of its output ports. The color-filled squares denote the frequency slot units (FSUs) occupied by the useful signals, while the empty ones represent the unfiltered, wasted slots. As the example illustrates, FONs suffer from a significant waste of spectrum and privacy issues due to the broadcasting and *drop-and-waste* transmission.

Fig. 1b depicts a ROADM-based WSON architecture, and a characteristic nodal setup with spectrum-selective switches (SSSs) in route&select configuration (shown for node 3 in the lower part of the figure). Naturally, this architecture does not suffer from any spectrum waste as all nodes filter the signals, but it is associated with a much higher cost of the nodes. As in FONs, WSON nodes also host a pre-amplifier and a booster at each ingress and egress port, respectively. Note that both FON and WSON nodes may host additional amplifiers at their *add* and *drop* sections. However, in our study, we focus only on the pass-through functionalities and do not consider the dimensioning of the *add* and *drop* segments.

The PFON architecture supporting the given set of demands is shown in Fig. 1c. Compared to Fig. 1a, PFON wastes less spectrum for unfiltered channels, implying a greater possibility of spectrum reuse than in FONs. The reduction in spectrum use is particularly noticeable on link 3–5, where the PFON uses 4 times fewer FSUs than the FON architecture. The detailed setup of nodes 3 and 4, shown in the bottom part of the figure, illustrates how the nodal architecture can be configured in a flexible manner, as per traffic requirements. AoD nodes support node bypass, often referred to as fiber switching, where an input and an output fiber are directly connected via the OB. In node 3, this allows for d_1 and d_2 to be sent from the incoming port from node 2 directly to the outgoing port towards node 6, while d_3 is added towards node 5. In node 4, fiber switching is not possible and d_4 and d_5 must be split before being directed to their corresponding output ports. Due to the absence of filtering, parts of each signal remain present on both split copies, represented by dashed lines. However, compared to the FON solution, fewer splitters/couplers are used and their degree is lower. Combined with fiber switching, this translates to a lower insertion loss and a lower number of used OB ports.

The existence of unfiltered signals and a lack of pre-defined nodal architecture in PFONs require tailored network design approaches. For a given physical topology of the optical network comprising nodes that host optical white box switches, interconnected with optical fiber links, and a given set of connection demands, the problem of designing a PFON considered in this paper comprises two intertwined sub-problems:

- Solving the routing, modulation and spectrum assignment (RMSA) problem for the offered traffic, taking into account the presence of unfiltered signals due to the *drop-and-waste* transmission. The RMSA problem is proven to be NP-complete already in WSONs [6], and is exacerbated by the presence of unfiltered signals.
- Determining the architecture of the nodes, i.e., the number and the type of components (passive couplers and EDFAs) to be deployed at the nodes, as well as the OB interconnections to support the required processing of the

traffic.

In [5], we carried out a preliminary study of the PFON architecture and formulated an integer linear program (ILP) for the RMSA problem in PFONs with the objective to minimize spectrum usage. Planning of PFONs based on space division multiplexing (SDM) was investigated in [7], while their feasibility was verified experimentally in [8]. However, cost-efficiency of the new architecture has not been studied so far. Low-cost, energy-efficient solutions require efficient use of active optical equipment at network nodes, i.e., EDFAs and OB switches in the AoD nodes, as well as high spectrum usage efficiency. Both of these parameters are strongly affected by the signal splitting. Splitting, combined with the absence of filtering, is the mechanism that generates spectrum waste. Splitting losses, which are a function of the splitter and coupler degrees, significantly contribute to the losses experienced by the signals inside PFON nodes, creating the need for EDFA deployment at nodes. Moreover, the required OB switch size (and the resulting cost) is directly proportional to the number and the degree of components it interconnects.

Therefore, in this work we extend upon our preliminary study from [5] and develop cost-efficient PFON planning approaches aimed at minimizing spectrum usage, the degree of deployed couplers, the number of required EDFAs, and the required size of the OB switching matrices. We formulate the RMSA problem for PFONs as an ILP with the objective to minimize the total degree of the deployed passive components and spectrum resource usage. The RMSA problem is NP-complete [6], so it is often decomposed into its constituent subproblems of routing, modulation format and spectrum assignment, as in, e.g., [9]. To avoid ILP scalability issues, we propose a two-step ILP formulation that allows finding near-optimal solutions for larger problem instances under short execution time. Furthermore, we propose a heuristic algorithm for the placement of EDFAs that computes the total loss experienced by each connection at each node and deploys the EDFAs required for intra-node loss compensation. We focus on the placement of amplifiers inside the nodes for node loss management purpose, assuming that the optical line system is already deployed and optimized for span loss management.

Our primary objective is to study the cost trade-offs related to the introduction of AoD-enabled programmability to filterless networks in terms of spectrum resource usage, as well as the OB switch and amplifier costs. A detailed simulation analysis carried out on two core and one regional network topology with varying total traffic indicates a strong potential of PFONs to achieve a favorable trade-off between spectral resource usage and equipment cost. The PFON architecture uses up to 64% less spectrum and up to 81% fewer EDFAs than the FON and WSON solutions with hard-wired node structure. On the other hand, PFON uses up to 66% more spectrum than WSON architecture, but reduces the need for optical switching equipment by up to 84% as it only uses 1 optical switch matrix per node instead of an SSS at each input and each output port of all ROADM nodes (considering route&select configuration).

The remainder of the paper is organized as follows. Section II reviews the related work on passive filterless networks and AoD as PFON enabling technologies. Section III presents the details of our proposed PFON design approaches whose performance is analyzed in Section IV, while Section V concludes the paper.

II. Related Work

A. Filterless Optical Networking

Since their original proposal in [10], passive filterless optical networks have been extensively studied through theoretical and experimental analysis. A detailed account of the FON concept, architecture, and design can be found in [11], along with an early validation of the FON physical-layer performance in [12]. Since then, extensive design and performance verification studies have established FONs as a viable option for cost-efficient core, metro and submarine networks.

The majority of the initial literature on FONs focused on their applications in core networks, addressing aspects related to design, resource assignment and operation. The problems of defining the node connectivity in the form of passive fiber trees and the static version of the routing and spectrum assignment (RSA) problem for fixed optical grid were addressed in [11], [13] for unprotected design, while [14] investigated 1+1 dedicated optical layer protection. Elastic FONs were introduced in [15], along with a heuristic approach for survivable RMSA with dedicated path protection. An in-depth study of the RMSA problem in FONs was carried out in [3] by developing an ILP formulation and a heuristic approach based on genetic algorithm (GA). Dynamic connection provisioning in FONs was addressed in [16] for terrestrial networks, while [17] investigated the resource savings benefits of dynamic connection reconfiguration under periodic traffic in filterless submarine networks. A control plane design based on path computation element (PCE) was proposed in [18]. Trial deployments in pilot networks based on FONs were carried out in Croatia (2012) and Germany (2014) [19]. Vendor-interoperable FONs interfaces were proposed and experimentally evaluated in [20], indicating great potential of this technology for open line systems.

Telecom operators' search for cost-efficient solutions that satisfy the proliferating traffic in metropolitan areas has been fueling the recent interest in filterless metro networks. [21] introduced a FON architecture for metro applications and developed a physical-layer model to assess their capacity and scalability. A FON node architecture that exploits bidirectional transmission over a single fiber was proposed in [22]. [23] proposed to double the capacity of filterless metro optical networks by exploiting the full C+L band, and implemented and validated extensions of the OpenConfig YANG model to support the C+L band FON transmission. Techno-economic aspects of filterless metro network solutions were studied in [24] and [25]. [24] defined a FON cost model and analyzed the savings with respect to WSONs, while [25] investigated software defined networking (SDN) as a dynamic and agile control plane for FONs.

In [26], the authors investigated the problem of virtual service chaining in filterless optical metro networks for dynamic traffic using a heuristic algorithm. [27] defined the

problem of survivable virtual network mapping (SVNM) in FONs, highlighting the differences from SVNM in WSONs and jointly solving the problems of fiber tree setup and SVNM with an ILP formulation. The work was extended in [28] by studying virtual network embedding with virtual link protection in FONs, while trying to minimize the network cost in terms of equipment and overall spectrum consumption.

Driven by the operators' interest to reduce equipment costs, the problem of amplifier placement in FONs has received substantial interest from different research groups lately. A GA-based approach for placing boosters, inline amplifiers, and pre-amplifiers in FONs with the objective of minimizing amplifiers cost by considering quality of transmission (QoT) parameters was proposed in [29]. In [30], the authors developed algorithms for the allocation of amplifiers and transponders and RSA in the open-source Net2Plan framework. The above efforts show that filterless networking is a widely considered solution with relevant applications in practical scenarios. A recent encompassing tutorial on FONs can be found in [31].

Upon the proposal of the PFON concept in [5], a limited number of studies evaluated them towards FONs and WSONs in terms of resource usage and cost. The authors in [32] proposed a traffic-adaptive exhaustive-search algorithm for reconfiguration of programmable optical switches in PFONs, with the sole objective of minimizing the overall spectrum consumption. In order to avoid spectrum waste generated by the *drop-and-waste* transmission, [7] proposed to combine PFONs with SDM technology where additional spatial dimensions are utilized to eliminate undesirable signal splitting. A heuristic algorithm for the routing, modulation format, spectrum, and core allocation (RMSCA) problem in programmable filterless SDM networks was proposed in [33], considering also the effect of inter-core crosstalk. Compared to the aforementioned approaches, we provide an ILP optimization framework for joint minimization of component usage and spectrum consumption in PFONs. We present a single-step joint optimization approach that obtains optimal solutions for smaller problem instances. Apart from considering spectrum usage, as in the existing models in the literature, our optimization approach considers the component cost as well, and aims at reducing the number of required EDFAs and the required size of the switch matrices in AoD nodes by minimizing the degree of the deployed passive couplers.

B. Optical White Boxes

Optical white boxes were proposed as a technological solution allowing for unprecedented flexibility in nodal architecture design and network provisioning [1]. The work in [1] analyzed the switching, routing and architectural flexibility of this technology, and experimentally demonstrated its feasibility and benefits. Procedures for synthesizing the nodal architecture to support a given traffic mapping between input and output ports of the node can be found in [34], [35]. The related analysis of scalability, power consumption and cost indicates a decrease in the number of used optical backplane ports and the resulting cost and power consumption due to aggregation of channels into fiber-switched port pairs that only use the optical backplane and bypass all other optical components in the node.

Cost-efficient network planning approaches for white box-based elastic networks under static and dynamic traffic were proposed in [36]. Their common objective is to dimension network nodes and perform RMSA for connection requests so as to minimize the number of used components. The impact of optical white box deployment to the availability of connections in the network was evaluated in [37], showing a strong reduction in network downtime due to the support of self-healing of node component failures. Cost-effective planning of AoD-based networks under static, multi-hour and dynamic traffic has been addressed in [38], [39], and [36], respectively. [40] investigated physical-layer implications of AoD and proposed optical signal-to-noise (OSNR)-aware procedures for nodal architecture composition. Advantages of AoD have been demonstrated in terms of scalability [36], energy efficiency [35], network reliability [37] and resilience [41].

Note that in all of these studies, optical white boxes were used to create complex AoD ROADM structures, where the optical backplane interconnects other active components such as SSSs, amplifiers, or sub-wavelength switches. However, in this paper we assume that the optical backplane uses only passive components to split or couple signals between different ports when necessary, as well as optical amplifiers for node loss compensation, without using any filtering components.

III. PFON Design: RMSA and Node Setup

A. Problem Definition

The RMSA problem in programmable filterless networks based on white boxes with the objective of minimizing spectrum usage, the need for amplifier deployment inside nodes, and the required OB switch matrix size can be formally defined as follows. Given a physical topology represented by a graph $\mathcal{G}(\mathcal{V}, \mathcal{E})$ comprising a set of nodes $\mathcal{V}$ and a set of links $\mathcal{E}$, and a set of traffic demands D, we must find a physical route through the network, select a modulation format and assign the appropriate number of spectrum slots to each demand. Moreover, we must determine the architecture of each node capable of supporting the devised routing solution by configuring an appropriate number and degree of passive couplers, and compensate for the incurred losses with EDFAs. When solving the RMSA problem, the spectrum continuity and contiguity constraints must hold, implying that a demand must use the same, adjacent, spectrum slots along all links included in its path, and there can be no spectrum overlapping among channels that carry useful signals and other useful or unfiltered signals generated due to *drop-and-waste* transmission. In our proposed approach, the objective of minimizing spectrum usage is modeled by minimizing the highest used FSU index in the network. The objective of reducing the component usage is modeled by minimizing the total degree of passive splitters/couplers deployed in the network.

B. Illustrative Example

The impact of route selection on the degree of deployed passive components and the subsequent need for amplification

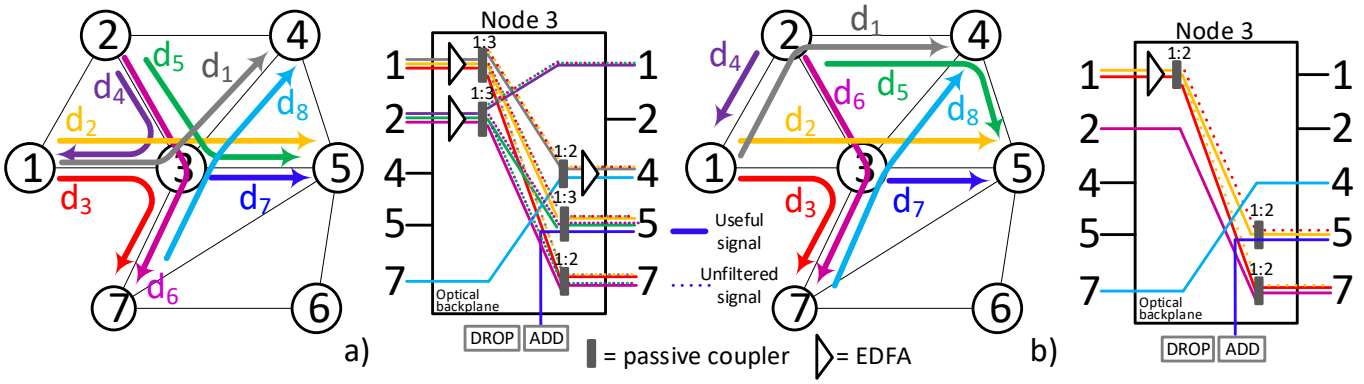

Figure 2. The impact of connection routing in programmable filterless networks on the architecture of node 3 and the necessary amplifiers without (a) and with trying to minimize signal splitting/coupling at node 3 (b).

is illustrated in Fig. 2 for two valid PFON solutions that serve a set of connections denoted with d_1–d_8, with a focus on the configuration of the central node 3.

The choice of routes used for each demand determine the necessary splitters and couplers. If connections d_i and d_j share the same incoming link to node v but are directed to different outputs, they need to be split at the ingress port. This is the case for, e.g., d_1, d_2 and d_3 in Fig. 2a, where a copy of each signal appears as unfiltered at the outgoing links of node 3 traversed by the other two connections. Analogously, if the two connections use the same outgoing link towards node u but arrive at node v via different incoming links, they need to be coupled at the egress port. This is the case for, e.g., d_3 and d_6 incoming to node 3 via links 1–3 and 2–3, respectively. In the proposed RMSA approach, our goal is to perform connection routing such that the resulting need for splitting/coupling (in terms of the total degree of the deployed passive couplers) is minimized.

Connection routing and the resulting deployment of passive couplers affect the required size of the OB switch and the need for amplification inside nodes. The required OB switch size is a function of the sum of the ports of all components that need to be deployed at the node. The deployment of amplifiers at PFON nodes depends on the total loss experienced by connections that traverse the node between the last line amplifier on the ingress link and the first line amplifier on the egress link. This encompasses the loss due to splitting, coupling and OB traversals inside the node, as well as attenuation on the last span of the ingress link and the first span of the egress link. Conventional node architecture assumes the deployment of pre-amplifiers and boosters at each ingress and egress port, respectively. In our design approach, we leverage on node architecture programmability to bypass the unnecessary amplifiers inside nodes, i.e., amplifiers whose absence yields signal power losses that can be compensated by other existing amplifiers inside the node or at the links.

A more detailed view of the components traversed by connection d_1 is shown in Fig. 3. The figure shows the line amplifiers on links 1–3 and 3–4, with highlighted distances l_1 and l_4. Inside each node, a connection passes through the OB switch as many times as needed to traverse the

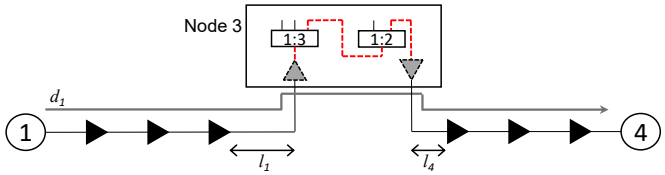

Figure 3. A detailed view of components traversed by connection d_1 inside PFON node 3. The amplifiers inside the node, shown in gray color, are deployed as needed, depending on the total losses generated due to splitting, OB switch traversals, and fiber attenuation on the last span of the ingress link and the first span of the egress link.

necessary components. Connections which undergo splitting and coupling at the node (e.g., d_1 in Fig. 2a) cross the OB three times, connecting *(i)* the input port of the node to the splitter, *(ii)* the splitter to the coupler, and *(iii)* the coupler to the output port of the node. These interconnections are denoted with red dashed lines in Fig. 3. Connections which bypass the node modules (e.g., d_8 in Fig. 2b) traverse the OB only once, to connect the input and the desired output port. If the loss experienced by a connection between the closest two line amplifiers at the ingress and egress link does not exceed an acceptable, predefined threshold that enables correct transmission, one or both amplifiers inside the node, depicted in gray color in Fig. 3, can be omitted.

To this end, for each connection, we calculate the total loss between the two closest amplification sites along the links incoming from and outgoing to the adjacent nodes. We assume the insertion loss of a passive 1:N coupler to be $L_{1:N}$=10log$N$, insertion loss per OB cross-connection of L_{OB}= 1 dB, amplifier input power threshold of -18 dBm, power at the amplifier output of 0 dBm per channel, and fiber attenuation coefficient of L_α=0.2 dB/km. For the example network from Fig. 2, distances l_i from node 3 to the first line amplifier along a link to/from the neighboring node i equal l_1=l_2=l_5=45 km, l_4=20 km, and l_7= 30 km.

For the solution in Fig. 2a, the total loss experienced by connection d_1 between the closest line amplifiers on the input fiber link from node 1 and on the output fiber link to node 4 equals $L_{d_1} = L_\alpha \cdot (l_1 + l_4) + L_{1:3} + L_{1:2} + 3 \cdot L_{OB}$ = 23.7 dB. This value is below the input power threshold of the first line

amplifier on link 3–4, so the connection must be amplified at node 3, as depicted in Fig. 3. The figure shows two amplifiers (i.e., at the input and the output port), which are needed to accommodate for the losses of other connections that use the same input and/or output ports of node 3 but traverse different paths through the network and/or different components inside the node (as shown in Fig. 2a).

Analogous to the above considerations, losses experienced by other connections between the two line amplifiers closest to node 3 equal L_{d_2}= 22.4 dB, L_{d_3}= 23.7 dB, L_{d_4}= 20.7 dB, L_{d_5}= 20.4 dB, L_{d_6}= 21.7 dB, L_{d_7}= 9.7 dB, L_{d_8}= 15 dB. Hence, d_1–d_6 must be amplified at node 3, resulting in a total of 3 used EDFAs, as shown in Fig. 2a. The solution in Fig. 2b applies a slightly different routing scheme, which results in a lower number and total degree of splitters at node 3. In this case, losses for d_2, d_3, d_6 and d_8 equal L'_{d_2}= 21 dB, L'_{d_3}= 24 dB, L'_{d_6}= 16 dB, L'_{d_8}= 11 dB, and a single deployed EDFA is sufficient to support d_2 and d_3. As the example also illustrates, lower degree of used passive splitters/couplers also reduces the propagation of unfiltered signals to unwanted output ports, thus reducing the overall spectrum waste.

C. Single-step ILP Formulation of the RMSA Problem in PFONs

The single-step ILP formulation for PFON design relies on the model from [5]. For consistency, we use similar notation in our formulation, but we simplify and modify it to enable calculation of the splitter and coupler degrees.

Input parameters

- $\mathcal{G}(\mathcal{V}, \mathcal{E})$: a directed graph with a set of nodes $\mathcal{V}$, and a set of links $\mathcal{E}$;
- D: set of traffic demands, where each element d is associated to traffic volume q_d from source node $s_d \in \mathcal{V}$ to destination node $t_d \in \mathcal{V}$;
- P: set of physical routes, where each element P_d defines a set of K available candidate physical routes $p^d \in P_d$ for demand $d \in \mathsf{D}$, and each route is associated with a number of needed FSUs F_{p^d} according to the modulation format selection method in [3];
- $\tau_{(p^d,p^{\hat{d}})}$: indicator for disjoint routes, equal to 0 when $p^d \in P_d$ and $p^{\hat{d}} \in P_{\hat{d}}$ are link disjoint, and 1 otherwise;
- $\Gamma_{(p^d,p^{\hat{d}})}$: set of links $\in p^{\hat{d}}$ unintentionally traversed by the established optical channel for d over path p^d due to the broadcasting via optical splitters;
- α, β: objective function weighting coefficients;
- T: a large constant.

Variables

- $x_{p^d} \in \{0,1\}$: equal to 1 if path $p^d \in P_d$ is used by $d \in \mathsf{D}$, and 0 otherwise;
- $f_d \in \mathbb{Z}^+$: the starting spectrum slot index for d;
- $S^v_{(\hat{u}v,vu)} \in \{0,1\}$: equal to 1 if any optical channel entering node $v \in \mathcal{V}$ via ingress link $(\hat{u}, v) \in \mathcal{E}$ is directed to the egress link (v, u), and 0 otherwise;
- $a^v_{(v,u)} \in \{0,1\}$: equal to 1 if there are demands added at node v and egressing towards node u, and 0 otherwise;
- $d^v_{(\hat{u},v)} \in \{0,1\}$: equal to 1 if there are demands ingressing from node $\hat{u}$ and dropped at node v, and 0 otherwise;
- $L^v_{\hat{u}v} \in \{0,1\}$: equal to 1 if a splitter is needed at the input port from node $\hat{u}$ of node v, and 0 otherwise.
- $L^v_{vu} \in \{0,1\}$: equal to 1 if a coupler is needed at the output port towards node u of node v, and 0 otherwise.
- $\Psi^{(d,\hat{d})}_{(p^d,p^{\hat{d}})} \in \{0,1\}$: equal to 1 if paths p^d and $p^{\hat{d}}$ are assigned to demands d and $\hat{d}$, respectively, and 0 otherwise;
- $\delta_{(d,\hat{d})} \in \{0,1\}$: equal to 0 if the starting slot number of d is greater than $\hat{d}$ (i.e., $f_d > f_{\hat{d}}$), and 1 otherwise;
- $\mathsf{C_i}^v_{(\hat{u},v)} \in \mathbb{Z}$: the degree of the splitter traversed by optical channels entering node v via ingress link $(\hat{u}, v)$;
- $\mathsf{C_o}^v_{(v,u)} \in \mathbb{Z}$: the degree of the coupler traversed by optical channels exiting node v via egress link (v, u);
- $\mathsf{M_s}$: the maximum allocated frequency slot unit (FSU) among all network links.

Objective function

$$\text{Minimize: } \alpha \cdot \mathsf{M_s} + \beta \cdot \sum_{v \in \mathcal{V}} \Big(\sum_{(\hat{u},v) \in \mathcal{E}} \mathsf{C_i}^v_{(\hat{u},v)} + \sum_{(v,u) \in \mathcal{E}} \mathsf{C_o}^v_{(v,u)} \Big) \quad (1)$$

Subject to

$$\sum_{p^d \in P_d} x_{p^d} = 1 \quad \forall d \in \mathsf{D} \quad (2)$$

$$\sum_{d \in \mathsf{D}} \sum_{p^d \in P_d : (\hat{u},v),(v,u) \in p^d} x_{p^d} \le \mathsf{T} \cdot S^v_{(\hat{u}v,vu)} \quad \forall v \in \mathcal{V}, \forall (\hat{u},v),(v,u) \in \mathcal{E} \quad (3)$$

$$\sum_{d \in \mathsf{D}: s_d = v} \sum_{p^d \in P_d : (v,u) \in p^d} x_{p^d} \le \mathsf{T} \cdot a^v_{(v,u)}, \forall (v,u) \in \mathcal{E} \quad (4)$$

$$\sum_{d \in \mathsf{D}: t_d = v} \sum_{p^d \in P_d : (\hat{u},v) \in p^d} x_{p^d} \le \mathsf{T} \cdot d^v_{(\hat{u},v)}, \forall (\hat{u},v) \in \mathcal{E} \quad (5)$$

$$\mathsf{T} \cdot L^v_{\hat{u}v} \ge \sum_{(v,u) \in \mathcal{E}} S^v_{(\hat{u}v,vu)} + d^v_{(\hat{u},v)} - 1, \quad (6)$$

$$2 \cdot L^v_{\hat{u}v} \le \sum_{(v,u) \in \mathcal{E}} S^v_{(\hat{u}v,vu)} + d^v_{(\hat{u},v)}, \quad \forall v \in \mathcal{V}, \forall (\hat{u},v) \in \mathcal{E}. \quad (7)$$

$$\mathsf{C_i}^v_{(\hat{u},v)} \ge \sum_{(v,u) \in \mathcal{E}} S^v_{(\hat{u}v,vu)} + d^v_{(\hat{u},v)} - \mathsf{T} \cdot (1 - L^v_{\hat{u}v}) \quad \forall v \in \mathcal{V}, \forall (\hat{u},v) \in \mathcal{E}. \quad (8)$$

$$x_{p^d} + x_{p^{\hat{d}}} - \Psi^{(d,\hat{d})}_{(p^d,p^{\hat{d}})} \le 1 \quad \forall (d,\hat{d}) \in \mathsf{D}, \forall p^d \in P_d, \forall p^{\hat{d}} \in P_{\hat{d}} \quad (9)$$

$$x_{p^d} + x_{p^{\hat{d}}} - 2 \cdot \Psi^{(d,\hat{d})}_{(p^d,p^{\hat{d}})} \ge 0 \quad \forall (d,\hat{d}) \in \mathsf{D}, \forall p^d \in P_d, \forall p^{\hat{d}} \in P_{\hat{d}} \quad (10)$$

$$f_{\hat{d}} - f_d \leq \mathsf{T} \cdot \delta^{(d,\hat{d})} - 1, \forall d, \hat{d} \in \mathsf{D} \tag{11}$$

$$f_{\hat{d}} - f_d \geq \mathsf{T} \cdot \delta^{(d,\hat{d})} - \mathsf{T}, \forall d, \hat{d} \in \mathsf{D} \tag{12}$$

$$f_d + \sum_{p^d \in P_d} F_{p^d} \cdot x_{p^d} - 1 \leq \mathsf{M_s} \quad \forall d \in \mathsf{D} \tag{13}$$

$$\begin{aligned} &f_d - f_{\hat{d}} + \mathsf{T} \cdot (\delta^{(d,\hat{d})} + \Psi^{(d,\hat{d})}_{(p^d,p^{\hat{d}})}) \leq 2 \cdot \mathsf{T} - F_{p^d} \\ &\forall (d,\hat{d}) \in \mathsf{D}, \forall p^d \in P_d, \forall p^{\hat{d}} \in P_{\hat{d}}, \tau_{(p^d,p^{\hat{d}})} = 1 \end{aligned} \tag{14}$$

$$\begin{aligned} &f_d - f_{\tilde{d}} + \mathsf{T} \cdot (\delta^{(d,\tilde{d})} + \Psi^{(d,\hat{d})}_{(p^d,p^{\hat{d}})} + x_{p^{\tilde{d}}}) \leq 3 \cdot \mathsf{T} - F_{p^d} \\ &\forall (d,\hat{d},\tilde{d}) \in \mathsf{D}, \forall p^d \in P_d, \forall p^{\hat{d}} \in P_{\hat{d}}, \forall p^{\tilde{d}} \in P_{\tilde{d}} : \Gamma_{(p^d,p^{\hat{d}})} \cap p^{\tilde{d}} \neq \{\emptyset\} \end{aligned} \tag{15}$$

$$\begin{aligned} &f_{\tilde{d}} - f_d + \mathsf{T} \cdot (\delta^{(\tilde{d},d)} + \Psi^{(d,\hat{d})}_{(p^d,p^{\hat{d}})} + x_{p^{\tilde{d}}}) \leq 3 \cdot \mathsf{T} - F_{p^{\tilde{d}}} \\ &\forall (d,\hat{d},\tilde{d}) \in \mathsf{D}, \forall p^d \in P_d, \forall p^{\hat{d}} \in P_{\hat{d}}, \forall p^{\tilde{d}} \in P_{\tilde{d}} : \Gamma_{(p^d,p^{\hat{d}})} \cap p^{\tilde{d}} \neq \{\emptyset\}, \end{aligned} \tag{16}$$

The objective (1) is to minimize the index of the maximum FSU used in the network $\mathsf{M_s}$ and the total degree of passive couplers deployed at network nodes. The weighting coefficients α and β allow for prioritization between the two contributions of the objective function according to the network operator preferences. Constraint (2) guarantees that a single route is assigned to each demand d. The degrees of passive splitters and combiners needed to route the optical channels in node v are determined by (3)–(8). (3)–(5) model the internal routing at node v for pass through, added and dropped connections, respectively. Exact splitter degrees are then calculated in (6)–(8) by modelling an *if-then-else* relationship between $\sum_{(v,u)\in\mathcal{E}} S^v_{(\hat{u}v,vu)} + d^v_{(\hat{u},v)}$ and $\mathsf{C}^v_{\mathsf{i}(\hat{u},v)}$, using $L^v_{\hat{u}v}$ as an auxiliary variable. If $\sum_{(v,u)\in\mathcal{E}} S^v_{(\hat{u}v,vu)} + d^v_{(\hat{u},v)} = 1$, which means that all connections entering node v from $\hat{u}$ either pass through towards the same node u or get dropped at v, then $\mathsf{C}^v_{\mathsf{i}(\hat{u},v)}$ needs to be 0 as no splitter is needed. If $\sum_{(v,u)\in\mathcal{E}} S^v_{(\hat{u}v,vu)} + d^v_{(\hat{u},v)} > 1$, which means that connections entering node v from $\hat{u}$ are directed towards different nodes u and/or get dropped at v, then $\mathsf{C}^v_{\mathsf{i}(\hat{u},v)}$ needs to be equal to that sum. An analogous procedure is carried out for each egress port of every node v in order to model the need for deploying couplers at each port and use it as an auxiliary variable to determine the exact degrees of the couplers $\mathsf{C}^v_{\mathsf{o}(v,u)}$.

Constraints (9)–(10) and (11)–(12) determine the values of $\Psi^{(d,\hat{d})}_{(p^d,p^{\hat{d}})}$ and $\delta^{(d,\hat{d})}$, respectively, needed for spectrum assignment. Spectrum contiguity is enforced by (13). Spectrum continuity and non-overlapping of the spectrum assigned to different traffic demands that share common link(s) are enforced by (14). (15) and (16) ensure that the spectrum slots occupied by unfiltered optical channels are not assigned to any other demand $\tilde{d}$.

Note that the above formulation can be conveniently transformed into the variant which only aims at minimizing spectrum usage without considering the splitter degrees. This transformation is carried out by eliminating the $\mathsf{C_i}$ and $\mathsf{C_o}$ from the objective function, and by omitting constraints (3)–(8).

D. Two-Step ILP Formulation of the RMSA Problem in PFONs

To reduce complexity and obtain sub-optimal results for realistic problem instances, we formulate a two-step ILP model for RMSA in PFONs. In the first step, the model tries to find a lower bound on the highest used spectrum slot index in the network through routing, without considering spectrum allocation to individual requests. After solving this step, the values of the x_{p^d} variables are set, and used as input for spectrum allocation in the second step.

Step 1: Spectrum-aware routing

In the first step, the model aims at solving the routing subproblem while avoiding the complexity associated with precise allocation of spectrum to individual requests. In addition to using the same variables related to connection routing as in the 1-step ILP model above, this phase introduces two additional variables:

- M^e_s: an estimate of the maximum used FSU index among all network links;
- $m_{(uv,p^d)} \in \{0,1\}$: an auxiliary variable whose value equals 1 if the unfiltered signal generated from p^d traverses link (u,v), and 0 otherwise.

Objective function

$$\text{Minimize: } \alpha \cdot \mathsf{M^e_s} + \beta \cdot \sum_{v\in\mathcal{V}} \Big(\sum_{(\hat{u},v)\in\mathcal{E}} \mathsf{C}^v_{\mathsf{i}(\hat{u},v)} + \sum_{(v,u)\in\mathcal{E}} \mathsf{C}^v_{\mathsf{o}(v,u)} \Big) \tag{17}$$

Subject to

Constraints (2)–(10)

$$\begin{aligned} K \cdot m_{(uv,p^d)} \geq \sum_{\hat{d}\in\hat{D}} \sum_{p\in p^{\hat{d}} \Gamma_{(p^d,p^{\hat{d}})} \cap p^{\tilde{d}} \neq \emptyset\}} \Psi_{(p^d,p^{\hat{d}})}, \\ \forall d, \in D, \forall p, \in p^d, \forall (u,v) \in \mathcal{E} \end{aligned} \tag{18}$$

$$\begin{aligned} m_{(uv,p^d)} \leq \sum_{\hat{d}\in\hat{D}} \sum_{p\in p^{\hat{d}} \Gamma_{(p^d,p^{\hat{d}})} \cap p^{\tilde{d}} \neq \emptyset\}} \Psi_{(p^d,p^{\hat{d}})}, \\ \forall d, \in D, \forall p, \in p^d, \forall (u,v) \in \mathcal{E} \end{aligned} \tag{19}$$

$$\begin{aligned} \sum_{d\in D} \sum_{p\in p^d, (u,v)\in p^d} x_{p^d} \cdot F_{p^d} + \sum_{d\in D} \sum_{p\in p^d} m_{(uv,p^d)} \cdot F_{p^d} \leq \mathsf{M^e_s}, \\ \forall (u,v) \in \mathcal{E} \end{aligned} \tag{20}$$

The objective of the routing step, given in (17), is to minimize the sum of the estimated value of the maximum used FSU index M^e_s and the total degree of passive couplers deployed at network nodes. The value of $m_{(uv,p^d)}$ is determined from

connection routing by (18) and (19), and used in (20) to approximate the maximum used FSU index on any link. The spectrum continuity and contiguity constraints are not considered in this phase, so an estimate on the maximum used FSU index is computed as the sum of the number of slots used to carry the traffic over any link and the slots used by unfiltered signals traversing that link. This represents a lower bound on the maximum FSU since the spectrum continuity and contiguity constraints lead to spectrum fragmentation.

Step 2: Spectrum assignment

After determining the routing and, consequently, the values of the x_{p^d} variables, the spectrum is allocated to the individual requests in the second step.

Objective function

Subject to

$$\text{Minimize: } \mathsf{M_s} \tag{21}$$

Constraints (11)–(12)

$$f_d + F_{p^d} - 1 \leq \mathsf{M_s}, \forall d \in D : x_{p^d} = 1 \tag{22}$$

$$\begin{gathered} f_d - f_{\hat{d}} + \mathsf{T}\cdot\delta^{(d,\hat{d})} \leq \mathsf{T} - F_{p^d}, \\ \forall (d,\hat{d}) \in \mathsf{D}, \forall p^d \in P_d, \forall p^{\hat{d}} \in P_{\hat{d}} : x_{p^d} = 1 \wedge x_{p^{\hat{d}}} = 1 \end{gathered} \tag{23}$$

$$\begin{gathered} f_d - f_{\tilde{d}} + \mathsf{T}\cdot\delta^{(d,\tilde{d})} \leq \mathsf{T} - F_{p^d}, \\ \forall (d,\hat{d},\tilde{d}) \in D, \forall p^d \in P_d, \forall p^{\hat{d}} \in P_{\hat{d}}, \forall p^{\tilde{d}} \in P_{\tilde{d}} : \\ \Gamma_{(p^d,p^{\hat{d}})} \cap p^{\tilde{d}} \neq \{\emptyset\} \wedge x_{p^d} = 1 \wedge x_{p^{\hat{d}}} = 1 \wedge x_{p^{\tilde{d}}} = 1 \end{gathered} \tag{24}$$

The objective of the spectrum assignment step, given by (21), is to minimize the maximum used FSU index in the network. A contiguous set of spectrum slots is allocated to each demand using (22). Constraint (23) avoids spectrum overlap among link-sharing demands and guarantee spectrum continuity. This constraint is analogous to (14) in the 1-step model. Constraint (24) avoids spectrum overlap of useful and unfiltered signals, replacing (15) and (16) from the 1-step model.

E. Complexity Analysis

The complexity of single-step ILP formulation in terms of the number of variables and constraints can be expressed as (25) and (26), respectively.

$$N_{var} = 4|\mathcal{V}|^2 + |\mathsf{D}|^2 \cdot (1 + \mathsf{K^2}) + |\mathsf{D}| \cdot (1 + \mathsf{K}) + |\mathcal{V}| \cdot |\mathcal{E}|^2 \tag{25}$$

$$\begin{aligned} N_{cnstr} = 2|\mathsf{D}| \cdot (1 + |\mathsf{D}|) + \mathsf{K}^2 \cdot |D|^2 \cdot (3 + 2\mathsf{K} \cdot |\mathsf{D}|) \\ + |\mathcal{V}| \cdot |\mathcal{E}| \cdot (\mathcal{E} + 3) \end{aligned} \tag{26}$$

To simplify the expressions, we can assume a fully-connected demand matrix where the number of demands and links grow linearly by $|\mathcal{V}|^2$. By considering the dominant factors, the number of variables and constraints can be approximated $N_{var} \approx |\mathcal{V}|^5 + K^2 \cdot |\mathcal{V}|^4$ and $N_{cnstr} \approx K^3 \cdot |\mathcal{V}|^6$, respectively.

The number of variables and constraints for the first step of the two-step ILP formulation are expressed in (27) and (28), respectively.

$$N_{var} = \mathsf{K}^2 \cdot |\mathsf{D}|^2 + |\mathcal{V}| \cdot |\mathcal{E}|^2 + 6|\mathcal{V}|^2 + \mathsf{K} \cdot |\mathsf{D}| \cdot (1 + |\mathcal{E}|) \tag{27}$$

$$N_{cnstr} = 2\mathsf{K}^2 \cdot |\mathsf{D}|^2 + |\mathcal{V}| \cdot |\mathcal{E}|^2 + 2\mathsf{K} \cdot |\mathsf{D}| \cdot |\mathcal{E}| + |\mathsf{D}| + 3|\mathcal{E}| \tag{28}$$

By following the same simplification assumptions as above, their complexity can be approximated by $N_{var} \approx |\mathcal{V}|^5 + K^2 \cdot |\mathcal{V}|^4$ and $N_{cnstr} \approx |\mathcal{V}|^5 + 2K^2 \cdot |\mathcal{V}|^4$, respectively. The main factor in reducing complexity is the lower number of constraints compared to the single-step ILP formulation.

Finally, the number of variables and constraints for the second step of ILP formulation can be expressed as (29) and (30), respectively.

$$N_{var} = 2|\mathsf{D}|^2 \tag{29}$$

$$N_{cnstr} = |\mathsf{D}|^3 + 3|\mathsf{D}|^2 + |\mathsf{D}| \tag{30}$$

After simplifying, they can be approximated as $N_{var} \approx 2|\mathcal{V}|^4$, and $N_{cnstr} \approx |\mathcal{V}|^6$. The strict conditions applied in (24) decrease the actual number of constraints which results in complexity reduction compared to the single-step ILP. In section IV-A, a comparison of the ILP execution times offers further insights into their run-time complexity.

F. Amplifier Placement

For the cost-minimizing RMSA solutions obtained by the ILP formulations, the placement of EDFAs is performed by computing the total loss experienced by each connection at each node, and deploying the EDFAs when necessary to compensate for these losses. Note that this work is concerned only by node architecture design, where our focus is on the placement of amplifiers inside nodes for node loss management purpose. We assume that the optical line system is already deployed and optimized for span loss management and that the launch channel power does not exceed the threshold for nonlinearities.

The pseudocode of the amplifier placement subroutine is shown in Algorithm 1. Fig. 4 shows the loss contributions considered during amplifier placement (we use the example of connection d_1 from Fig. 3). The amplifier placement algorithm takes as input the network topology $\mathcal{G}(\mathcal{V}, \mathcal{E})$, the routing solution R, the line amplifier output power P_{out} and input power threshold P_{in}, the insertion losses of the OB switch L_{OB} and the deployed $1{:}N$ couplers $L_{1:N}$, as well as the fiber attenuation L_α.

For each network node v, the algorithm processes the physical routes p_d of all demands d that traverse node v (lines

Algorithm 1: Amplifier placement procedure.

Data: $\mathcal{G}(\mathcal{V},\mathcal{E})$, R, P_{out}, P_{in}, L_{OB}, $L_{1:N}$, L_{α}.
Result: Placement of amplifiers at each node.

1 $P_{budget} = P_{out} - P_{in}$;
2 **for** $v = 1$ ***to*** $|\mathcal{V}|$ **do**
3 **for** $p_d = 1$ ***to*** $|\mathsf{R}|$ *s.t.* $v \in p_d$ **do**
4 $\hat{u} \leftarrow$ predecessor of v in p_d;
5 $u \leftarrow$ successor of v in p_d;
6 $L \leftarrow$ loss of d between the last amplifier on link ($\hat{u}$,v) and the used output port of v;
7 $\overline{L} \leftarrow$ loss of d between the used input port of v and the first amplifier on link (v,u);
8 $L_{TOT} \leftarrow$ total loss of d between last amplifier on ($\hat{u}$,v) and first amplifier on (v,u);
9 **if** $L_{TOT} > P_{budget}$ **then**
10 **if** $L > P_{budget}$ ***and*** $\overline{L} > P_{budget}$ **then**
11 Place amplifier at used input and output ports of v;
12 **if** $L > P_{budget}$ ***and*** $\overline{L} \leq P_{budget}$ **then**
13 Place amplifier at used input port of v;
14 **if** $L \leq P_{budget}$ ***and*** $\overline{L} > P_{budget}$ **then**
15 Place amplifier at used output port of v;
16 **if** $L \leq P_{budget}$ ***and*** $\overline{L} \leq P_{budget}$ **then**
17 Place amplifier at used input/output port with a higher degree coupler; or at input if both couplers are of same degree;

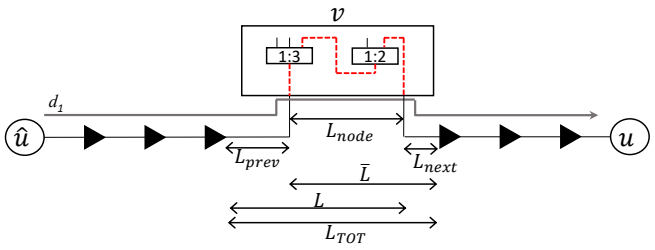

Figure 4. Loss contributions considered during amplifier placement.

2-3). First, the predecessor and successor nodes in path p_d are identified, denoted as $\hat{u}$ and u, respectively (lines 4-5). Then, the loss contributions for each traversed components are calculated, as illustrated in Fig. 4 for connection d_1 and node $v = 3$.

L denotes the loss between the last amplification site on the ingress link $(\hat{u}, v)$ and the output of node v. It is calculated as the sum of fiber attenuation on link $(\hat{u}, v)$, denoted as L_{prev}, and the internal node loss L_{node}. Analogously, $\overline{L}$ refers to the losses between the input of node v and the first line amplifier on link (v, u). It is calculated as the sum of L_{node} and fiber attenuation on the first span of link (v, u), denoted as L_{next}. L_{TOT} measures the total loss between the two closest line amplifiers at the ingress and egress links of node v. If L_{TOT} exceeds the power budget P_{budget} between these two line amplifiers (line 9), the signal requires extra amplification at the node. In case both L and $\overline{L}$ exceed P_{budget}, an amplifier must be placed at the input and at the output port of node v associated to links $(\hat{u}, v)$ and (v, u) (lines 10-11). Otherwise, one amplifier is sufficient and its placement is determined as follows. If only the value of L exceeds P_{budget}, an amplifier is placed at the input port of node v connecting it to node $\hat{u}$ (lines 12-13). Conversely, if only $\overline{L}$ exceeds the threshold, an amplifier is placed at the output port of v connecting it to u (lines 14-15). In case both L and $\overline{L}$ are below the P_{budget} threshold, the necessary amplifier can be added at either of the two ports. In this case, the port that hosts a passive coupler of a higher degree is chosen, whereas the input port is selected if the two degrees are the same (lines 16-17).

IV. Numerical Results

We evaluate the performance of the proposed single-step and two-step ILPs for the cost-efficient PFON design in terms of spectrum and component usage. Spectrum consumption considerations refer to the highest used FSU index in the network and the portion of spectrum wasted due to *drop-and-waste* transmission. Component usage considerations include the number and the degree of used passive couplers, the number of used EDFAs and the maximum size of the deployed OB switch matrix.

The results used in the analysis are obtained via simulations on the German and the Italian backbone networks, and a realistic regional network denoted as Reference network 1 [3]. The topologies are shown in Fig. 5 and their characteristics are summarised in Table I. Each link is assumed to comprise one fiber per direction supporting 320 FSUs and additional fibers can be deployed in case capacity is exceeded [3]. Links are equipped with pre-deployed line amplifiers that compensate for the span losses. Adopting a similar approach as in [42], we assume even spacing of line amplifiers, whose value is varied in the analysis. We consider a multi-period scenario with 5 traffic periods of increasing traffic for the German and Italian networks, and 3 traffic periods for Reference network 1 [3]. At every period, the traffic volume is distributed among each node pair and direction in a non-uniform way as in [3]. We assume that each source-destination pair combines all the traffic volume in one direction into a single demand $d \in D$. Unless otherwise stated, we assume that reconfiguration is performed during the transition between traffic periods, i.e., the model is solved independently for each period. The weighting coefficients α and β are set to 1, which allows for balancing the two contributions of the same order of magnitude.

In Sec. IV-A, we first compare the results obtained by the single-step and two-step ILP formulations for smaller problem instances, i.e., the smallest, German topology and lighter network traffic load. All solutions are obtained using the Gurobi 7.5 solver [43] using 4 CPUs per problem instance, running on a server with 2.1 GHz Intel Xeon CPU and 128 GB of RAM. The results obtained by the single- and the two-step model for the PFON architecture are denoted as PF-RSA and PF-R+SA, respectively.

We then analyze the performance of the two-step ILP on larger problem instances in Sec. IV-B, comparing the proposed PFON solutions to FON and WSON benchmarks. The WSON solutions, denoted as WSON-RSA and WSON-R+SA for the equivalent single- and two-step approaches,

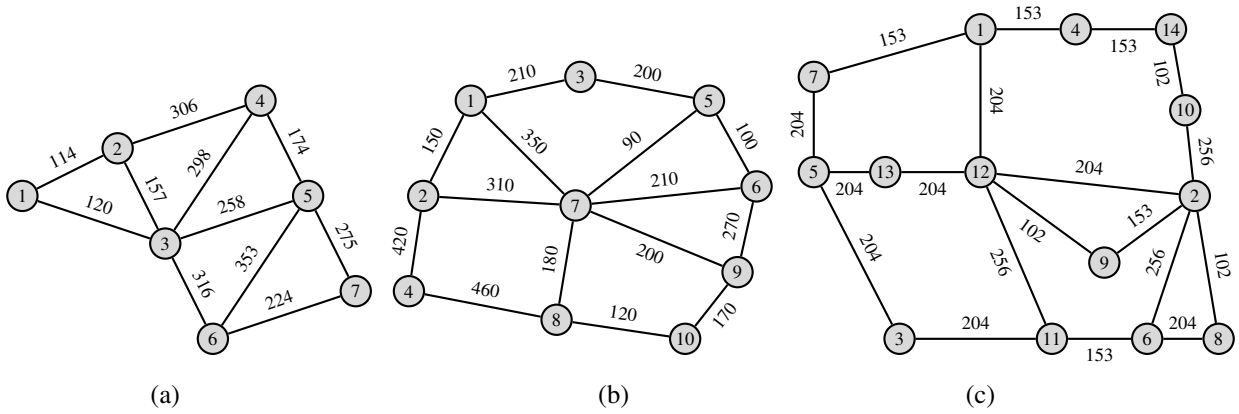

Figure 5. The German (a), the Italian (b) and the Reference network 1 topology (c) used in the simulations. The number next to each link indicates its length in km.

Table I
CHARACTERISTICS OF NETWORK TOPOLOGIES

Topology	Nodes	Links	Average nodal degree
German network	7	11	1.57
Italian network	10	15	1.5
Reference network 1	14	19	1.35

Table II
SUMMARY OF OPTIMIZATION MODELS

Abbreviation	Model
FON	Filterless optical networks solution
WSON-RSA	Single-step ILP solution for WSON
WSON-R+SA	Two-step ILP solution for WSON
PF-RSA	Single-step ILP solution for PFON
PF-R+SA	Two-step ILP solution for PFON
PF-SM-RSA	Spectrum minimizing single-step ILP solution for PFON
PF-SM-R+SA	Spectrum minimizing two-step ILP solution for PFON
PF-R+SA-TD	Two-step ILP solution for PFON with traffic domination

were obtained by modifying the ILP from Sec. III-C to omit the PFON-related variables and constraints. For example, the modified single-step ILP formulation for WSON minimizes the maximum used spectrum slot (21) and uses constraints (2) and (13)–(14). The baseline FON solutions are obtained by the heuristic from [3] for scalability reasons. We also compare the proposed multi-criteria PFON solutions to those aimed only at spectrum minimization (i.e., setting α=1 and β=0 to disregard component usage), denoted as PF-SM-RSA and PF-SM-R+SA for the single-step and two-step approach, respectively.

Finally, we consider a scenario without reconfiguration between traffic periods to model the case where complete reprogramming of optical nodes is not desirable by a network operator. Hence, an approach based on total traffic domination, inspired by [44] and denoted as PF-R+SA-TD, is introduced and tested on the German network topology. This approach optimizes connection routing (i.e., runs the first step of the two-step ILP) only once, for the traffic period with the largest total traffic demand. The resulting routing and node configuration are applied to serve the demands in earlier traffic periods, while allowing only for the optimization of the spectrum (obtained by solving the second step of the two-step ILP) in each period. All models and their abbreviations are summarized in Table II.

A. Single-step and Two-step ILP Comparison

To assess the quality of the sub-optimal solutions obtained by the two-step ILP formulation, we compare them to the optimal solutions of the single-step ILP. Due to the prohibitively high complexity of the single-step ILP approach, optimal results could only be obtained for smaller-sized problem instances, i.e., those with a lower traffic load. To this end, we only use the German network topology serving half of the requests from the traffic matrices, i.e., 21 connection request serving 43.5 Tbit/s of total traffic for the highest load.

Fig. 6a shows the maximum FSU index used by the single- and two-step ILPs for PFON and WSON architectures. The optimal PF-RSA solution obtains, on average, only 1.6% lower maximum FSU than the sub-optimal two-step approach PF-R+SA. This advantage equals 1.7% for the variant where only spectrum usage is minimized (see PF-SM-RSA vs. PF-SM-R+SA) and 2.8% for the case of WSON (see WSON-RSA vs. WSON-R+SA), which indicates strong potential of the two-step approach to obtain solutions of very high quality. Depending on the traffic load, the PF-RSA solutions use between 10% and 18% more spectrum than WSON-RSA, and the trend is analogous for the two-step approach.

Fig. 6b shows the sum of the degrees of passive devices used for the single- and two-step ILPs solutions. Here, too, the two approaches have very close performance, with a $< 1\%$ gap on average over all traffic periods. However, differences are observable between the single- and multi-objective versions of the models. Since the single-objective variant does not consider the degree of the passive components, it tends to yield a higher total degree than the variant which considers it jointly with the spectrum. Overall, the spectrum-only minimizing ILP approaches tend to obtain on average 7% lower maximum FSU usage than those that consider the more complex objective,

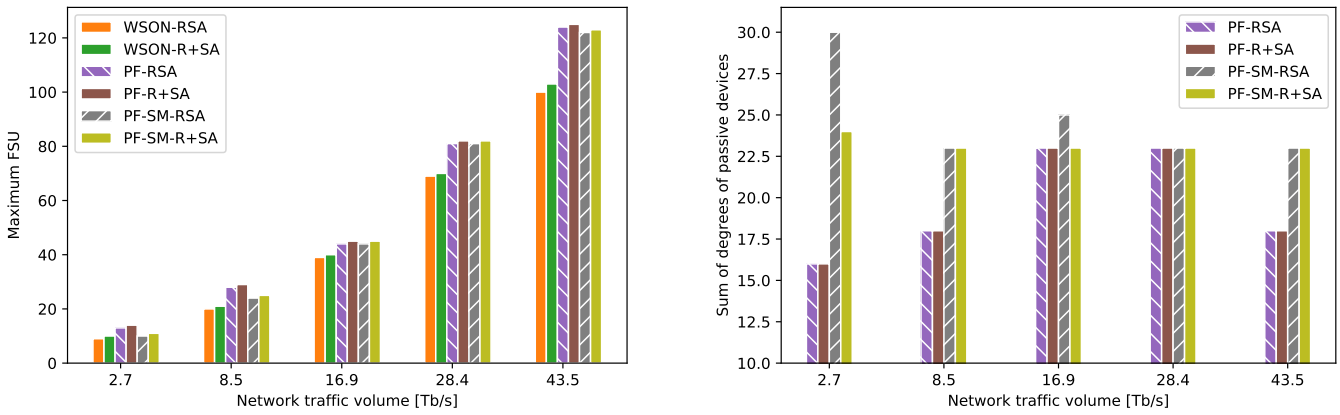

(a) Maximum used frequency slot unit (FSU)

(b) Sum of the degrees of passive devices

Figure 6. Single-step (RSA) and two-step (R+SA) ILP comparison for 21 traffic demands in the German network.

Table III
SOLVING TIMES OF THE ILP FORMULATIONS

Solution	Run time	
	21 demands	42 demands
WSON-RSA	16 minutes	13.87 days
WSON-R+SA	0.14 second	13.79 seconds
PF-RSA	4.2 days	28 days (non-optimal)
PF-R+SA	0.46 second	0.62 hours
PF-SM-RSA	3.6 hours	28 days (non-optimal)
PF-SM-R+SA	0.218 second	12.74 hours

at the expense of 16% higher average degree of the used components.

Table III compares the execution times of the single-step and two-step ILP formulation as an indicator of their runtime complexity. Apart from the instances with 21 request examined above, we test the approaches on a set of problem instances with full connectivity (i.e., 42 connection requests) to impose a greater strain on the ILPs. Results confirm the much lower complexity of the two-step model, which permits its applicability to problem instances of realistic sizes. In some cases, the execution of the single-step ILPs was terminated after 28 days without finding the optimal solution. In cases when both formulations were solved to the optimum, the two-step one was solved in 4 to 5 orders of magnitude shorter time than the single-step one. For example, the running time of PF-R+SA with 21 demand was $7.9 \cdot 10^5$ times shorter than that of PF-RSA. The above analysis shows that the two-step ILP formulation can find near-optimal solutions within a much shorter time than the single-step ILP.

B. Comparison of PFONs, FONs and WSONs

To evaluate the resource usage of PFONs, we compare the proposed two-step ILP with FON and WSON architectures under fully-connected traffic matrices for different network topologies. Figs. 7a, 7b, and 7c show the highest used FSU index for the different design strategies and a varying traffic load for the German, Italian network, and Reference network 1, respectively. The PFON architecture drastically reduces the spectrum usage compared to FONs. On average over all traffic scenarios for the German topology, PF-R+SA and PF-SM-R+SA use 43% and 45% less spectrum than the FON solution, respectively. The same trend is observed for the larger topologies. For the Italian network, the PF-R+SA and PF-SM-R+SA schemes both use 38% less spectrum than FON on average. The analogous reduction over FON obtained by the two approaches for the Reference 1 network is 59% and 64%, respectively. The average overhead in spectrum usage compared to WSON solutions is 43% and 42% (German network), 66% and 65% (Italian network), and 66% and 61% for the PF-R+SA and PF-SM-R+SA schemes, respectively. The observed performance trends can be motivated as follows. In networks with lower connectivity, such as the Reference 1 topology, FON solutions have the highest spectrum usage for similar traffic loads compared to the more connected topologies, which can be explained with low flexibility in fiber tree design and connection routing. There, the PFON solutions obtain the most significant advantage over FON. Conversely, in topologies with higher connectivity, such as the German network, PFON again leverages greater flexibility in node configuration and route selection and achieves the lowest spectrum usage overhead over WSON architecture. This confirms the premise that the programmable filterless network represents a good compromise solution between passive filterless and filtered, wavelength-switched optical networks in terms of spectrum consumption.

A deeper insight into the amount of spectrum wasted due to the *drop-and-waste* transmission is provided by Fig. 8. We express it as the ratio between the number of FSUs occupied by unfiltered channels and the total utilized number of FSUs. The PFON solutions waste significantly less spectrum than FON, where PF-R+SA and PF-SM-R+SA yield 44% and 36% lower spectrum dissipation on average over all network topologies, respectively. These results also reveal that the joint consideration of splitting and spectrum minimization leads to more efficient spectrum usage through the reduction of spectrum waste.

The extent of unwanted distribution of signals to unintended

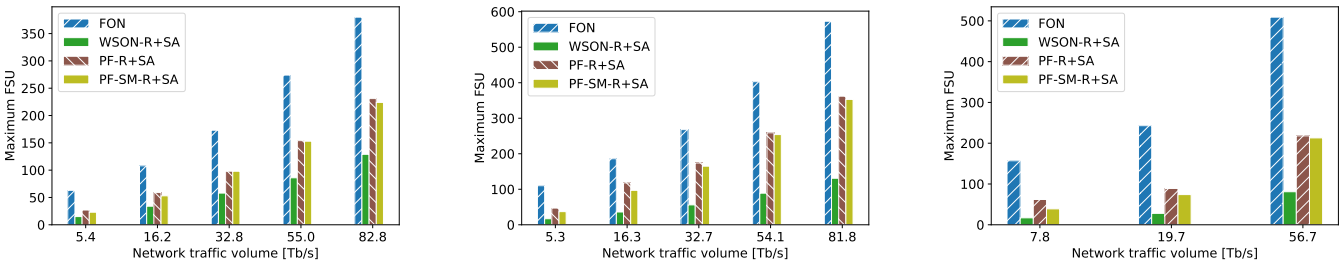

(a) German network (b) Italian network (c) Reference network 1

Figure 7. The maximum used frequency slot unit (FSU) for the three networks.

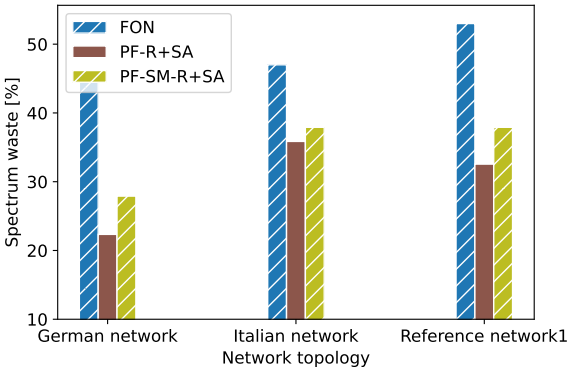

Figure 8. The average percentage of wasted spectrum for the three networks over all traffic periods.

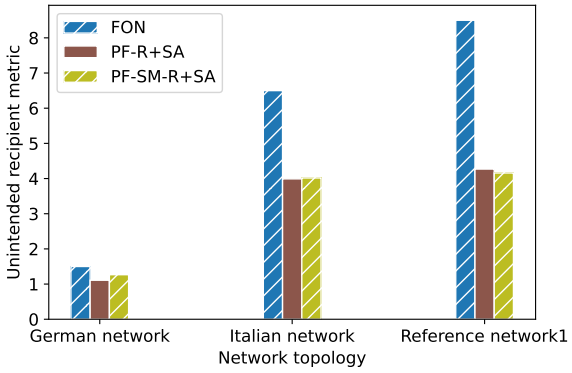

Figure 9. The average unintended recipient metric for the three networks.

destinations in PFONs and in FONs is compared in Fig. 9. We define a metric which we refer to as the unintended recipient metric, calculated as the ratio between the number of nodes that receive unwanted signals via unfiltered spectrum and the total number of demands. In a passive tree of N nodes, each demand will be unintentionally received by $(N-2)$ nodes (i.e., all nodes in the tree except the source and the intended destination), so this metric for the FON solutions based on fiber trees can be calculated as a constant. As can be seen in the figure, PFON reduces the average extent of unwanted broadcasting in the network by 21%, 39% and 50% compared to FON for the three considered networks, respectively. Further reduction of this metric could be achieved by incorporating it into the ILPs as an objective or a constraint, which is beyond the scope of this paper. Moreover, combining the programmable filterless architecture with SDM can in some cases completely eliminate unwanted signal broadcast, as shown in [7].

In the following, we analyse the component usage performance of the proposed approach. Fig. 10, shows the sum of the degrees of passive couplers deployed in the three networks on average over the traffic periods. In all cases, the multi-objective PF-R+SA outperforms PF-SM-R+SA. PF-R+SA decreases the value of this parameter by 16% compared to PF-SM-R+SA for the German topology, whereas the average value of the highest FSU index used by the two approaches over all traffic periods (shown in Fig. 7) are within 5% difference. The reduction in the sum of coupler degrees obtained by PF-R+SA is 14% for the Italian and 17% for the Reference network 1, at a spectrum usage overhead of 7% and 10%, respectively, compared to PF-SM-R+SA. These values indicate that jointly optimizing spectrum usage and splitter degree reduces spectrum waste without adversely affecting the maximum FSU usage.

Fig. 11 shows the total number of EDFAs deployed at network nodes by the considered approaches in the highest loaded traffic scenario for the three networks. To investigate the impact of line amplifier spacing and input power thresholds, we consider the scenarios with amplifier spacing values of 60, 75, and 100 km, and amplifier input power thresholds of -12, -15 and -18 dBm, as reported in the literature (e.g., [45]). The nodes in FONs and WSONs are hard-wired, with pre-amplifiers and boosters placed at each ingress and egress port, as shown in Fig. 1. Therefore, the number of deployed EDFAs in those architectures is fixed, and shown with a red dashed line in the figures. The PFON solutions require significantly fewer amplifiers than FON/WSON. The proposed PF-R+SA design approach performs the best in all considered settings. The advantages for the German topology are the greatest under amplifier spacing of 60 km and input power threshold of -18 dBm, where the PF-R+SA requires 80% fewer EDFAs at network nodes than FON/WSON. In Reference network 1, PF-R+SA obtains the greatest advantage for the 100 km amplifier spacing, where it decreases the number of amplifiers by 81% compared to both FON and WSON under the input power threshold of -18 dBm. This can be explained by the

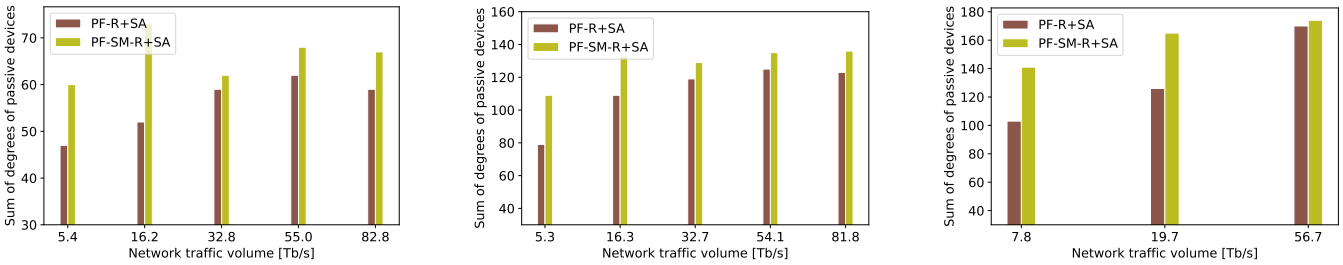

(a) German network (b) Italian network (c) Reference network 1

Figure 10. The average sum of the degrees of passive couplers deployed in the three networks over all traffic periods.

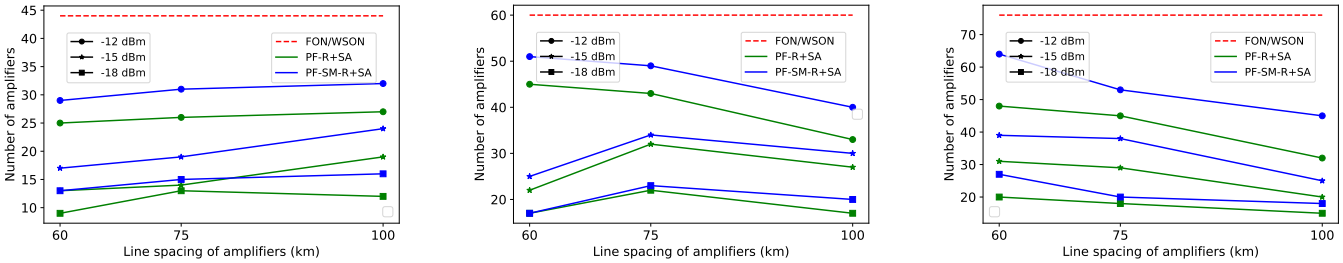

(a) German network (b) Italian network (c) Reference network 1

Figure 11. The total number of amplifiers used at the nodes for the three networks, for varied line amplifier spacing and input power threshold.

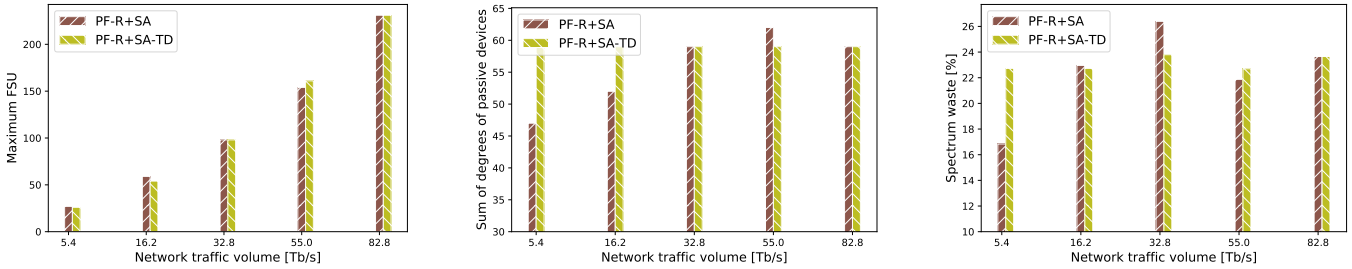

(a) Maximum frequency slot unit (FSU) (b) Sum of the degrees of passive couplers (c) Wasted spectrum

Figure 12. Comparison of period-independent and traffic domination approaches for the German topology.

fact that there are 8 links with a length of 204 km and line amplifiers are installed close to the nodes of those links. The savings in nodal amplifier deployment are enabled by a reduction in the degree of passive splitters that lowers the insertion losses, combined with the relatively short distances between the last line amplifier on the incoming link and the first line amplifier on the outgoing link. As lower splitting degrees also create less unfiltered signals, the proposed PFON design brings considerable savings in terms of EDFA usage while maintaining low spectrum consumption.

On average over all amplifier threshold and placement scenarios, PF-R+SA reduces the number of amplifiers used at network nodes by 60%, 52%, and 62% compared to FON/WSON for the German, Italian, and Reference networks, respectively. It also uses 19%, 11% and 21% fewer amplifiers than PF-SM-R+SA on average, respectively.

The number and the size of switching components required to support the PFON and WSON solutions for different network topologies is reported in Table IV. The modest OB switch matrix dimensions indicate a strong advantage of the PFON architecture in terms of the cost of active switching components compared to the conventional WSON architecture. Namely, each ROADM node of degree d would require d SSSs in broadcast&select configuration, and $2d$ in route&select configuration. A PFON node, on the other hand, only requires one OB switch matrix to support the required functionalities. This results in an 84%, 83% and 82% reduction of the number of used optical switches for the three network topologies compared to a route&select WSON, respectively.

Finally, Figs. 12a, 12b, and 12c show the highest used FSU index, the sum of the degrees of passive couplers, and the spectrum waste for the period-independent planning scheme and the traffic domination approach in the German network, respectively. The sum of coupler degrees of PF-R+SA-TD for all traffic volumes is the same since connection routing and node configuration of the highest-loaded traffic period (traffic

Table IV
USAGE OF OPTICAL SWITCHES FOR THE DIFFERENT TOPOLOGIES

Network topology	Maximum OB switch size for PFON	Number of OB switches for PFON	Number of SSSs for WSON
German	20 × 20 (node 3)	7	44
Italian	34 × 34 (node 7)	10	60
Reference 1	32 × 32 (node 12)	14	76

demand 5) are used in the other periods as well. The results reveal minor variations in the coupler degree sum (Fig. 12b) and spectrum waste (Fig. 12c) in the first traffic period, but no substantial difference between PF-R+SA and PF-R+SA-TD in terms of the highest used FSU. This indicates the potential of the proposed approach to maintain good performance while being attuned to an operator's needs, priorities and practical limitations.

V. CONCLUSION

The paper proposed a detailed design framework for programmable filterless optical network (PFON) architecture based on coherent elastic transmission and optical white box switches. The routing, modulation format and spectrum assignment problem in these networks was combined with the node architecture design problem and formulated as an integer linear program with the objective of minimizing spectrum usage and passive coupler degrees. To cope with the prohibitive complexity of the joint formulation, the problem was decomposed into two consecutive steps, allowing to obtain near-optimal solutions in drastically shorter time. Compared to passive filterless optical networks (FONs), the proposed PFON architecture decreases the highest used spectrum slot index by up to 64%, reduces the spectrum waste by up to 44%, and lowers the average extent of unwanted signal broadcasting in the network by up to 50%. Compared to conventional wavelength-switched optical networks (WSONs), PFON uses down to only 16% of the total number of optical switches at a trade-off with increased spectrum usage and reduces the number of optical amplifiers at network nodes by up to 81% compared to FON/WSON. This indicates the potential of the proposed programmable filterless architecture to obtain agile, flexible solutions at a fraction of WSON cost and FON spectrum usage.

REFERENCES

[1] N. Amaya, G. Zervas, and D. Simeonidou, "Introducing node architecture flexibility for elastic optical networks," *IEEE/OSA J. Opt. Commun. Netw.*, vol. 5, no. 6, pp. 593–608, June 2013.

[2] Polatis, "Series 6000n network optical switch," 2022. [Online]. Available: {https://www.hubersuhner.com/en/products-en/fiber-optics/optical-switches/polatis-optical-switches/series-6000}

[3] E. Archambault, N. Alloune, M. Furdek, Z. Xu, C. Tremblay, A. Muhammad, J. Chen, L. Wosinska, P. Littlewood, and M. P. Bélanger, "Routing and spectrum assignment in elastic filterless optical networks," *IEEE/ACM Trans. Netw.*, vol. 24, no. 6, pp. 3578–3592, December 2016.

[4] N. Sambo *et al.*, "Next generation sliceable bandwidth variable transponders," *IEEE Commun. Mag.*, vol. 52, no. 2, pp. 163–171, February 2015.

[5] M. Furdek, A. Muhammad, G. Zervas, N. Alloune, C. Tremblay, and L. Wosinska, "Programmable filterless network architecture based on optical white boxes," in *ONDM*, 2016.

[6] K. Christodoulopoulos, I. Tomkos, and E. A. Varvarigos, "Elastic bandwidth allocation in flexible OFDM-based optical networks," *Journal of Lightwave Technology*, vol. 29, no. 9, pp. 1354–1366, 2011.

[7] A. Muhammad, M. Furdek, G. Zervas, and L. Wosinska, "Filterless networks based on optical white boxes and SDM," in *ECOC*, 2016.

[8] G. M. Saridis, B. J. Puttnam, R. S. Luis, W. Klaus, T. Miyazawa, Y. Awaji, G. Zervas, D. Simeonidou, and N. Wada, "Experimental demonstration of a flexible filterless and bidirectional SDM optical metro/inter-DC network," in *ECOC*, 2016.

[9] L. Velasco, M. Klinkowski, M. Ruiz, and J. Comellas, "Modeling the routing and spectrum allocation problem for flexgrid optical networks," *Photonic Netw. Commun.*, vol. 24, no. 3, pp. 177–186, 2012.

[10] C. Tremblay, F. Gagnon, B. Châtelain, E. Bernier, and M. P. Bélanger, "Filterless optical networks: A unique and novel passive WAN network solution," in *OECC/IOOC*, 2007, pp. 466–467.

[11] E. Archambault, D. O'Brien, C. Tremblay, F. Gagnon, M. P. Bélanger, and E. Bernier, "Design and simulation of filterless optical networks: Problem definition and performance evaluation," *IEEE/OSA J. Opt. Commun. Netw.*, vol. 2, no. 8, pp. 496–501, August 2010.

[12] J. P. Savoie, C. Tremblay, D. V. Plant, and M. P. Bélanger, "Physical layer validation of filterless optical networks," in *ECOC*, 2010, p. P5.08.

[13] B. Jaumard, Y. Wang, and D. Coudert, "Dantzig–Wolfe decomposition for the design of filterless optical networks," *Journal of Optical Communications and Networking*, vol. 13, no. 12, pp. 312–321, 2021.

[14] Z. Xu, E. Archambault, C. Tremblay, J. Chen, L. Wosinska, M. P. Bélanger, and P. Littlewood, "1+1 dedicated optical-layer protection strategy for filterless optical networks," *IEEE Commun. Lett.*, vol. 18, no. 1, pp. 98–101, January 2014.

[15] Z. Xu, C. Tremblay, E. Archambault, M. Furdek, J. Chen, L. Wosinska, M. P. Bélanger, and P. Littlewood, "Flexible wavelength assignment in filterless optical networks," *IEEE Commun. Lett.*, vol. 18, no. 14, pp. 565–568, April 2015.

[16] P. Littlewood, M. P. Belanger, C. Tremblay, M. Nooruzzaman, and N. Alloune, "Network resource optimization based on time-varying traffic in optical networks," U.S. Patent 10 623 126B2, 2020.

[17] M. Nooruzzaman, N. Alloune, C. Tremblay, P. Littlewood, and M. P. Bélanger, "Resource savings in submarine networks using agility of filterless architectures," *IEEE Communications Letters*, vol. 21, no. 3, pp. 512–515, 2017.

[18] G. Mantelet, C. Tremblay, D. V. Plant, P. Littlewood, and M. P. Bélanger, "PCE-based centralized control plane for filterless networks," *IEEE Commun. Mag.*, vol. 51, no. 1, pp. 44–51, January 2014.

[19] A. Clauberg, "IPv6 deployment in Germany and Croatia," 2012, [Online]. [Online]. Available: \url{http://www.ipv6observatory.eu/wp-content/uploads/2012/11/01-06-Axel-Clauber1.pdf}

[20] M. Gunkel, A. Mattheus, F. Wissel, A. Napoli, J. Pedro, N. Costa, T. Rahman, G. Meloni, F. Fresi, F. Cugini, N. Sambo, and M. Bohn, "Vendor-interoperable elastic optical interfaces: Standards, experiments, and challenges [invited]," *IEEE/OSA J. Opt. Commun. Netw.*, vol. 7, no. 12, pp. B184–B193, December 2015.

[21] D. Uzunidis, E. Kosmatos, C. Matrakidis, A. Stavdas, and A. Lord, "DuFiNet: Architectural considerations and physical layer studies of an agile and cost-effective metropolitan area network," *IEEE/OSA J. Opt. Commun. Netw.*, vol. 99, no. PP, pp. 1–7, December 2018.

[22] D. Uzunidis, M. Presi, A. Sgambelluri, F. Paolucci, A. Stavdas, and F. Cugini, "Bidirectional single-fiber filterless optical networks: modeling and experimental assessment," *Journal of Optical Communications and Networking*, vol. 13, no. 6, pp. C1–C9, 2021.

[23] F. Paolucci, R. Emmerich, A. Eira, N. Costa, J. Pedro, P. W. Berenguer, C. Schubert, J. Fischer, F. Fresi, A. Sgambelluri *et al.*, "Disaggregated edge-enabled C+L-band filterless metro networks," *IEEE/OSA Journal of Optical Communications and Networking*, vol. 12, no. 3, pp. 2–12, 2019.

[24] O. Karandin, O. Ayoub, F. Musumeci, and M. Tornatore, "A techno-economic comparison of filterless and wavelength-switched optical metro networks," in *International Conference of Transparent Optical Networks*, 2020, pp. 1–4.

[25] P. Pavon-Marino, F.-J. Moreno-Muro, M. Garrich, M. Quagliotti, E. Riccardi, A. Rafel, and A. Lord, "Techno-economic impact of filterless data plane and agile control plane in the 5G optical metro," *Journal of Lightwave Technology*, vol. 38, no. 15, pp. 3801–3814, 2020.

[26] L. Askari, O. Ayoub, F. Musumeci, and M. Tornatore, "On dynamic service chaining in filterless optical metro-aggregation networks," *IEEE Access*, vol. 8, pp. 222 233–222 241, 2020.

[27] O. Ayoub, A. Bovio, F. Musumeci, and M. Tornatore, "Survivable virtual network mapping in filterless optical networks," in *2020 International Conference on Optical Network Design and Modeling (ONDM)*. IEEE, 2020, pp. 1–6.

[28] O. Ayoub, L. Askari, A. Bovio, F. Musumeci, and M. Tornatore, "Virtual network mapping vs embedding with link protection in filterless optical networks," in *GLOBECOM 2020-2020 IEEE Global Communications Conference*. IEEE, 2020, pp. 1–6.

[29] M. Ibrahimi, O. Ayoub, O. Karandin, F. Musumeci, A. Castoldi, R. Pastorelli, and M. Tornatore, "Qot-aware optical amplifier placement in filterless metro networks," *IEEE Communications Letters*, vol. 25, no. 3, pp. 931–935, 2020.

[30] P. Pavon-Marino, M. Garrich, F. J. Moreno-Muro, M. Quagliotti, E. Riccardi, A. Rafel, and A. Lord, "Hands-on demonstration of open-source filterless-aware offline planning and analysis tool for WDM networks," in *2020 Optical Fiber Communications Conference and Exhibition (OFC)*, 2020, pp. 1–3.

[31] O. Ayoub, O. Karandin, M. Ibrahimi, A. Castoldi, F. Musumeci, and M. Tornatore, "Tutorial on filterless optical networks [invited]," *J. Opt. Commun. Netw.*, vol. 14, no. 3, pp. 1–15, Mar 2022.

[32] O. Ayoub, F. Fatima, A. Bovio, F. Musumeci, and M. Tornatore, "Traffic-adaptive re-configuration of programmable filterless optical networks," in *ICC 2020-2020 IEEE International Conference on Communications (ICC)*. IEEE, 2020, pp. 1–6.

[33] V. Abedifar and M. Eshghi, "Routing, modulation format, spectrum and core allocation in space-division-multiplexed programmable filterless networks," *Optical fiber technology*, vol. 49, pp. 37–49, 2019.

[34] M. Garrich, N. Amaya, G. S. Zervas, J. R. F. Oliveira, P. Giaccone, A. Bianco, D. Simeonidou, and J. C. R. F. Oliveira, "Architecture on demand design for high-capacity optical SDM/TDM/FDM switching," *IEEE/OSA J. Opt. Commun. Netw.*, vol. 7, no. 1, pp. 21–35, January 2015.

[35] M. Džanko, M. Furdek, B. Mikac, G. Zervas, E. Hugues-Salas, and D. Simeonidou, "Synthesis, resiliency and power efficiency of function programmable optical nodes," in *ConTEL*, 2015.

[36] A. Muhammad, G. Zervas, N. Amaya, D. Simeonidou, and R. Forchheimer, "Introducing flexible and synthetic optical networking: Planning and operation based on network function programmable ROADMs," *IEEE/OSA J. Opt. Commun. Netw.*, vol. 6, no. 7, pp. 635–648, July 2014.

[37] M. Džanko, M. Furdek, G. Zervas, and D. Simeonidou, "Evaluating availability of optical networks based on self-healing network function programmable ROADMs," *IEEE/OSA J. Opt. Commun. Netw.*, vol. 6, no. 11, pp. 974–987, November 2014.

[38] M. Furdek, M. Džanko, N. Skorin-Kapov, and L. Wosinska, "Planning of optical networks based on programmable ROADMs," in *ACP*, 2015.

[39] M. Furdek, M. Džanko, M. Matanic, I. Boric, L. Wosinska, and B. Mikac, "Multi-hour network provisioning utilizing function programmable ROADMs," in *ICTON*, 2015.

[40] H. Liu, A. Peters, M. Garrich, and G. Zervas, "OSNR-aware composition of an open and disaggregated optical node and network," *IEEE/OSA J. Opt. Commun. Netw.*, vol. 9, no. 10, pp. 844–854, October 2017.

[41] M. Džanko, B. Mikac, and M. Furdek, "Dedicated path protection for optical networks based on function programmable nodes," *Opt. Switch. Netw.*, vol. 27, pp. 79–87, January 2018.

[42] M. Ibrahimi, O. Ayoub, F. Musumeci, O. Karandin, A. Castoldi, R. Pastorelli, and M. Tornatore, "Minimum-cost optical amplifier placement in metro networks," *Journal of Lightwave Technology*, vol. 38, no. 12, pp. 3221–3228, 2020.

[43] Gurobi Optimization, LLC, "Gurobi Optimizer Reference Manual," 2021. [Online]. Available: https://www.gurobi.com

[44] R. Aparicio-Pardo, N. Skorin-Kapov, P. Pavon-Marino, and B. Garcia-Manrubia, "(Non-)reconfigurable virtual topology design under multi-hour traffic in optical networks," *IEEE/ACM Transactions on Networking*, vol. 20, no. 5, pp. 1567–1580, 2012.

[45] O. Karandin, O. Ayoub, M. Ibrahimi, F. Musumeci, A. Castoldi, R. Pastorelli, and M. Tornatore, "Optical metro network design with low cost of equipment," in *2021 International Conference on Optical Network Design and Modeling (ONDM)*, 2021, pp. 1–4.